JACS
JOURNAL OF THE AMERICAN CHEMICAL SOCIETY
Article
pubs.acs.org/JACS

Iridium-Catalyzed, Intermolecular Hydroamination of Unactivated Alkenes with Indoles

Christo S. Sevov,[†,‡] Jianrong (Steve) Zhou,[‡] and John F. Hartwig*[,†,‡]

[†]Division of Chemical Sciences, Lawrence Berkeley National Laboratory, Department of Chemistry, University of California, Berkeley, California 94720

[‡]Department of Chemistry, University of Illinois, 600 South Mathews Avenue, Urbana, Illinois 61801, United States

Supporting Information

ABSTRACT: The addition of an N−H bond to an olefin is the most direct route for the synthesis of alkylamines. Currently, intermolecular hydroamination is limited to reactions of a narrow range of reagents containing N−H bonds or activated alkenes, and all the examples of additions to unactivated alkenes require large excesses of alkene. We report intermolecular hydroamination reactions of indoles with unactivated olefins. The reactions occur with as few as 1.5 equiv of olefin to form *N*-alkylindoles exclusively and in good yield. Characterizations of the catalyst resting state, kinetic data, labeling studies, and computational data imply that the addition occurs by olefin insertion into the Ir−N bond of an *N*-indolyl complex and that this insertion reaction is faster than insertion of olefin into the Ir−C bond of the isomeric C-2-indolyl complex.

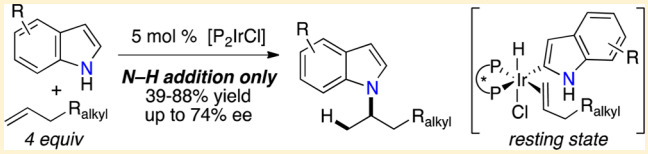

INTRODUCTION

Nitrogen-containing heterocycles constitute many biologically active and medicinally important compounds.[1−3] The indole core is one of the most prevalent architectures found in these compounds.[4] As a result, extensive effort has been dedicated to developing new strategies for site-selective functionalization of the indole ring.[5−7] However, participation of the lone pair on nitrogen in the aromatic system makes indoles more nucleophilic at C3 than at the nitrogen. Thus, in the absence of deactivating groups,[8] intermolecular alkylation of indoles selectively at nitrogen remains challenging.[9]

Classical methodologies for the alkylation of amines involve substitution reactions of aliphatic electrophiles or reductive amination of carbonyl compounds.[10] However, the scope of these processes does not include reactions of indoles. Brønsted or Lewis acid catalyzed formation of *N*-vinylindoles that could undergo reduction is often slow, and indole polymerization is common under these conditions. Furthermore, indoles are often competitively reduced to indolines under hydridic conditions.[11] Finally, nucleophilic substitution with secondary alkyl electrophiles leads to hydrodehalogenation or competitive alkylation at the C3 position of indole (Scheme 1).[12]

Alternatively, one could envision forming *N*-alkyl indoles by hydroamination: the formal addition of an N−H bond across an unsaturated C−C bond. Such addition reactions would exploit the abundance of alkene starting materials to form products with complete atom economy, but these reactions do not occur without a catalyst.[13] Metal-catalyzed hydroamination with indole as the N−H donor has the potential to form *N*-alkyl rather than *C*-alkyl indole products in a single step with chemo-, regio-, or stereochemical control; however, there are no examples of additions of indole N−H bonds to unactivated alkenes.

Catalytic hydroamination has been studied by many researchers,[14−16] but hydroaminations of unactivated alkenes are limited in scope. Most reported hydroaminations are intramolecular cyclizations of aminoalkenes.[17−23] With few exceptions,[24−30] intermolecular hydroamination is limited to reactions of activated alkenes, such as bicycloalkenes,[31−34] vinylarenes,[35−38] allenes,[39,40] or dienes,[41,42] or to reactions of ethylene.[43−45] Hydroaminations of unactivated alkenes are conducted with solvent quantities or large excesses of the alkene and are limited to amides,[30] cyclic ureas,[28] sulfonamides,[26,27] or cyclopentyl- and benzylamines.[29] The prevalence of indole cores in biologically active molecules renders indoles an important, yet unexplored, class of substrates for hydroamination.[4] Furthermore, synthesis of *N*-alkylindoles by olefin hydroamination, instead of reaction with an alkyl electrophile, could occur selectively at the N−H bond over the nucleophilic C3 position. These reactions would provide valuable mechanistic data on reactions of N−H bonds of azoles with organometallic complexes and subsequent addition to olefins.

We report iridium-catalyzed additions of the N−H bond of indoles to unactivated α-olefins. In contrast to the reactions of strained alkenes, which form the products from C−H addition

Scheme 1. Common Challenges to Traditional Alkylation Protocols of Indoles at Nitrogen

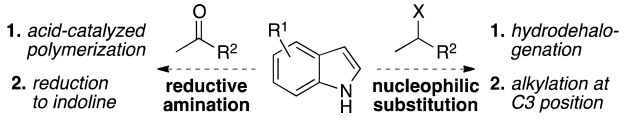

Received: November 27, 2013
Published: February 2, 2014

dx.doi.org/10.1021/ja412116d | J. Am. Chem. Soc. 2014, 136, 3200−3207

Scheme 2. Ir-Catalyzed C−H vs N−H Bond Addition to Olefins

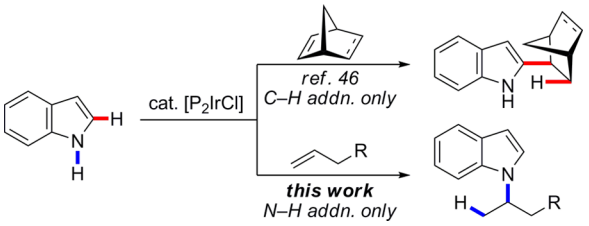

of indole (Scheme 2, top),[46] the reactions of indole with unstrained α-olefins formed exclusively the products of N−H addition (Scheme 2, bottom). These N−H addition reactions require as few as 1.5 equiv of olefin and form *N*-alkylindole products in good yield. Experimental mechanistic studies reveal information about the effect of ligand on the structure of the catalyst resting state. A combination of experimental and computational studies indicates that the barrier to insertion of alkenes into the Ir−N bond of an indolyl complex is lower than that for insertion into the Ir−C bond of the tautomer and imply that the turnover-limiting step is olefin insertion into an Ir−N bond.

RESULTS AND DISCUSSION

Method Development. The reactions of the indole N−H bond with an α-olefin under a variety of conditions are shown in Table 1. Previously, we showed that Ir complexes of DTBM-Segphos (DTBM = 3,5-di-*tert*-butyl-4-methoxyphenyl) catalyze the hydroheteroarylation of bicycloalkenes with indoles.[46] In contrast, the combination of $[Ir(cod)Cl]_2$ (cod =1,5-cyclooctadiene) and a series of bisphosphine ligands as catalyst led to the addition of the indole N−H bond to 1-octene in varying yields. In all cases, the reaction occurred exclusively at the N−H bond with Markovnikov selectivity to form **1**, along with smaller amounts of oxidative amination product **1-ene**. The reaction occurred with substantial enantiomeric excess (70% at 80 °C, vide infra), a result that rules out hydroamination of the alkene by a proton-catalyzed process alone. Trace amounts of octane were detected, suggesting that 1-octene is the terminal oxidant for the process that forms **1-ene**.

Reactions conducted with Ir complexes of Segphos or DM-Segphos (DM = 3,5-dimethylphenyl) formed products in low yield at 150 °C (Table 1, entries 1 and 2). Much higher reactivity was observed when the bulky DTBM analogue of Segphos was used as ligand (entry 3). The selectivity for **1** over **1-ene** was higher when the reaction was conducted at 100 °C instead of 150 °C, but **1** was formed in only 45% yield, due to slow rates and low conversion (entry 5 vs 3). Various solvents were tested to increase the reaction rate at 100 °C, but reactions in most solvents occurred to lower conversion.

However, an increase in the reaction rates and yields were observed when the reactions were conducted with added EtOAc. A plot of the conversion vs the amount of added EtOAc is given in Figure 1. These data show that this promoting effect of the ester is the largest with 1 equiv of EtOAc, relative to the indole (Table 1, entry 8), and smaller at higher concentrations of EtOAc.

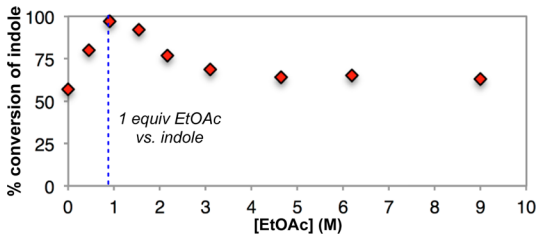

Figure 1. Effect of added EtOAc on reaction conversion after 18 h with 0.9 M initial indole concentration.

The reaction conducted with 1 equiv of added EtOAc proceeded with a 1.6-fold higher initial rate than the reaction conducted in the absence of EtOAc. The origin of its positive effect on reaction rate is unknown at this time; the added EtOAc was not consumed during the reaction. Nevertheless, since this protocol involved added EtOAc, the yields of reactions at 100 °C were comparable to those of reactions conducted at 150 °C without EtOAc, and smaller amounts of **1-ene** formed.

Scope of Olefin Hydroamination with Indoles. The scope of addition of the N−H bond of a range of indoles to 1-octene by the procedure just described is illustrated in Chart 1. The products from addition of indoles containing benzyl- or

Table 1. Reaction Development for the Ir-Catalyzed N−H Bond Addition of Indole to 1-Octene[a]

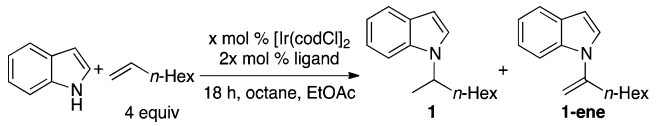

entry	ligand	*x* mol % $[Ir(cod)Cl]_2$	temp (°C)	EtOAc (equiv)	% **1**	% **1-ene**	**1/1-ene**
1	(*S*)-SEGPHOS	1	150	0	9	7	1.3
2	(*S*)-DM-SEGPHOS	1	150	0	15	5	3.0
3	(*S*)-DTBM-SEGPHOS	1	150	0	74[b]	23	3.2
4	(*S*)-DTBM-SEGPHOS	2	120	0	72	20	3.6
5	(*S*)-DTBM-SEGPHOS	2	100	0	45	11	4.1
6	(*S*)-DTBM-SEGPHOS	2	100	10	50	13	3.8
7	(*S*)-DTBM-SEGPHOS	2	100	5	52	13	4.0
8	**(*S*)-DTBM-SEGPHOS**	**2**	**100**	**1**	**76**[c]	**18**	**4.2**
9	(*S*)-DTBM-SEGPHOS	2	100	0.5	63	16	3.9
10[d]	(*S*)-DTBM-SEGPHOS	4	80	1	65[e]	12	5.4

[a]Yields were determined by GC analysis. [b]20% ee. [c]64% ee. [d]48 h reaction time. [e]70% ee.

dx.doi.org/10.1021/ja412116d | *J. Am. Chem. Soc.* 2014, 136, 3200−3207

Chart 1. Ir-Catalyzed Additions of Indoles to 1-Octene[a]

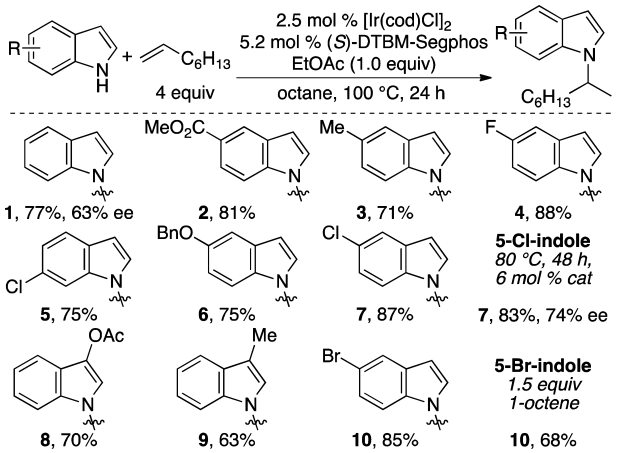

[a]Reported yields are isolated yields.

acetyl-protected alcohols, esters, and halides were formed in good yield. No products formed from reactions of indoles with substituents at the 2- or 7-positions, but electron-donating or -withdrawing substituents at the 3-position were tolerated (products **8** and **9**). The electron density of the indole ring had little influence on the final yield, but reactions of electron-poor indoles proceeded with higher rates than reactions of electron-rich indoles. The limits on the temperature at which the reaction can be performed and the amount of olefin that can be used were tested. The addition of 5-chloroindole to octene occurred at just 80 °C. Under these conditions, compound **7** was generated in a high 83% yield with 74% ee. The reaction conducted with 1.5 equiv of 1-octene at 100 °C formed **10** in 68% yield.

The scope of alkene that undergoes the addition reaction is summarized in Chart 2. Products from additions to olefins containing bulky substituents near the alkene moiety were generally formed in lower yields than those from additions to 1-octene. In these reactions, significant amounts of vinylindole side products were formed (20% to 30%), and isomerization of the terminal alkene to unreactive internal olefin isomers was observed for reactions of allyl cyclohexane (entry **12**, 15% terminal alkene remains). Good yields of product were obtained with bulky alkenes by conducting the reaction with up to 8 equiv of olefin. Reactions conducted with these higher concentrations of alkene required up to 2 equiv of EtOAc to achieve an increase in the reaction rate that equals the increase observed for additions to the less hindered 1-octene (see the Supporting Information for conditions specific to each substrate).

Chart 2. Ir-Catalyzed Addition of Idoles to α-Olefins[a]

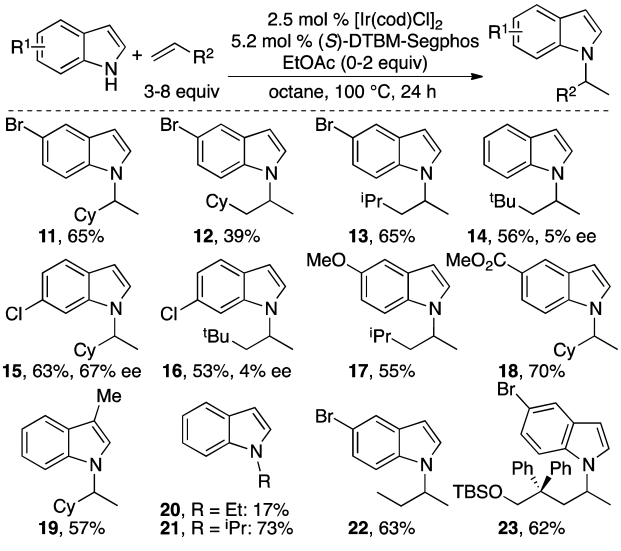

[a]Reported yields are isolated yields.

Ir-catalyzed addition to gaseous alkenes was achieved with only 4 equiv of ethene, propene, or butene (entries **20**–**22**). Reactions of indole and ethene proceed to complete conversion, but they formed **20** in poor yield as a result of competitive reaction at the C2 position of indole. In contrast, additions to propene and butene occurred exclusively at nitrogen.

Mechanistic Studies of Olefin Hydroamination with Indoles. Intermolecular hydroamination of unactivated alkenes remains challenging, and reactions are generally conducted with large excesses of olefin. However, little mechanistic data are available that provides insight into that challenges associated with additions to this class of olefin. Our studies on the scope of α-olefin hydroamination with indoles has revealed that reactions can be conducted with as few as 1.5 equiv of alkene, and reactions occur at temperatures as low as 80 °C. Mechanistic study of this mild reaction, relative to other NH additions to unactivated alkenes, could provide information about the properties of the catalytic system that promote hydroamination. Thus, we conducted experimental mechanistic studies and computational studies on the reported reactions.

Isotope Labeling Experiments. We began our mechanistic investigation by measuring the enantiomeric excess (ee) with which the addition product is formed. The ee of the products from a range of Ir-catalyzed additions of indoles to α-olefins were not exceptional but were substantial (45–74%, see the Supporting Information for details). In contrast to reactions of alkenes that are linear or have a tertiary branch point, the ee's of the product from the reaction of indoles with *tert*-butylpropene were only 4–5% ee (Chart 2: see **1** vs **14** or **15** vs **16**).

Scheme 3. Ir-Catalyzed Additions of D-Indole to Olefins

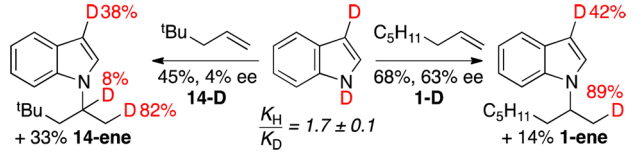

An isotope-labeling experiment was conducted to gain insight into the mechanism of N–H bond addition across an alkene, potential side reactions, and the origin of the large differences in ee for the two classes of alkenes. The addition of 1,3-dideuterioindole to 1-octene formed **1-D** with deuterium located exclusively β- to nitrogen (Scheme 3, right). However, addition to *tert*-butylpropene formed **14-D** with measurable amounts of deuterium α- to nitrogen (Scheme 3, left). Furthermore, a larger amount of oxidative amination product was generated from *tert*-butylpropene than from octene. Incorporation of deuterium α- to nitrogen in the product from *tert*-butylpropene likely occurs by hydrogenation of the vinylindole product by an Ir–D complex.

dx.doi.org/10.1021/ja412116d | J. Am. Chem. Soc. 2014, 136, 3200–3207

To determine the effect of this reduction of the vinylindole on stereoselectivity, we determined the absolute configuration of the products from hydroamination and vinylindole reduction. The absolute stereochemistry of the major enantiomer of representative hydroamination product **22** was determined to be 2*S* by single-crystal X-ray diffraction of the crystalline derivative **24** (eq 1). Reductive workup of

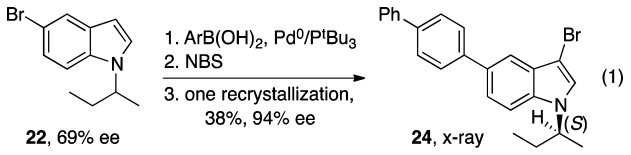

vinylindole **1-ene** with ^{i}PrOH catalyzed by the Ir complex remaining in solution converted **1-ene** into **1**. Quantitative conversion of **1-ene** was observed, but this reduction of **1-ene** formed the opposite enantiomer of **1** than did the hydroamination reaction. These data suggest that a significant amount of **14** may be generated in low ee from unselective reduction of **14-ene** in situ. A similar correlation was observed during our study on the addition of amides to α-olefins.[30] The reactions of amides produced alkyl amide products with poor ee, along with equimolar amounts of eneamide products.

Mechanism of C−N Bond Formation. Iridium-catalyzed C−H and N−H additions to bicycloalkenes have been shown to occur by olefin insertion into an Ir−C[46] or Ir−N[47,34,30] bond, respectively. Alternatively, hydroaminations of α-olefins catalyzed by late-transition-metal complexes have been proposed to occur by nucleophilic attack on a coordinated olefin ligand.[44,26,28] Moreover, palladium-catalyzed oxidative amination of alkenes occurs by both *syn*- and *anti*-aminopalladation of the olefin.[48−53] Given the different chemoselectivity of Ir-catalyzed indole addition to bicycloalkenes (C−H addition) versus α-olefins (N−H addition), the mechanism of C−N bond formation in Ir-catalyzed additions to α-olefins was studied.

To distinguish between the pathways described above, the geometry of the vinylindole products from reactions with geometrically defined alkenes was determined. The Ir-catalyzed reaction was performed with indole and (*E*)-octene-1-d_1 (Figure 2a). After 24 h, a 1:1 ratio of *E* and *Z* isomers of **1-ene** had formed. When the reaction was monitored at lower conversions, **(*E*)-1-ene** was observed as the major vinylindole isomer (Figure 2b). These results suggest that **(*E*)-1-ene** is the product of the initial Ir-catalyzed reaction, while the *Z* isomer is formed by isomerization of the *E* isomer. The formation of **(*E*)-1-ene** as the kinetic product is consistent with a mechanism involving migratory insertion of (*E*)-octene-1-d_1 into an Ir−N bond, followed by stereospecific syn-coplanar β-H elimination, as illustrated in Figure 2c.

Characterization of the Resting State Ir Complexes. The mode by which the indole binds to the catalyst was determined by synthesis of potential intermediates and was unexpected. The reaction of DTBM-Segphos, $[Ir(cod)Cl]_2$, with 1 equiv of indole and 10 equiv of 1-octene cleanly formed a complex with corresponding NMR signals matching those of the major species observed during catalytic reactions. This complex was characterized by NMR spectroscopy in solution and was shown to be complex **25**, the product of C−H activation at the C2 position of indole (eq 2). An Ir(deuteride) resonance was observed by ^{2}H NMR spectroscopy when a similar experiment was conducted with 2-indole-d_1, a result that

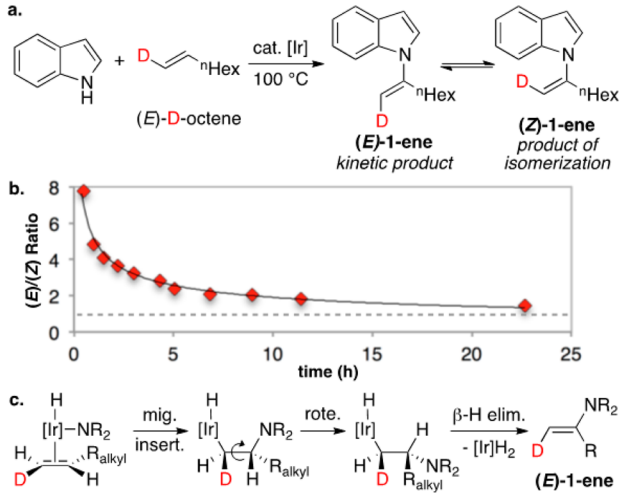

Figure 2. (a) Ir-catalyzed addition of indole to (*E*)-D-octene. (b) Ratio of **(*E*)-1-ene** to **(*Z*)-1-ene** vs time. (c) Proposed mechanism for the stereospecific formation of **(*E*)-1-ene**.

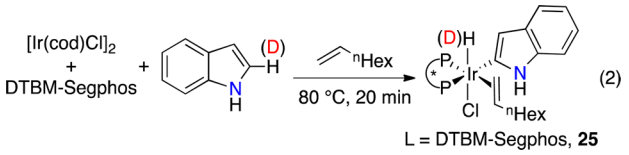

further supports a carbon- rather than nitrogen-bound indolyl group in the catalyst resting state. Correlations between ligand ^{31}P atoms and upfield-shifted vinylic protons were observed in the ^{31}P−^{1}H HMBC NMR spectrum, indicating that the sixth ligand of the octahedron is 1-octene. Although this complex contains a carbon-bound indolyl ligand, heating the solution of **25** to 100 °C for 2 h formed *N*-alkyl products **1** and **1-ene** in a combined yield of 94%. No product from reaction at the C2 position of indole was observed.

The high solubility of **25** prevented isolation in pure form. Thus, we conducted similar stoichiometric reactions with more polar Segphos derivatives that also formed catalysts for the addition of the indole N−H bond to α-olefins, albeit less active catalysts than those containing DTBM-Segphos. In contrast to stoichiometric studies with Ir complexes of DTBM-Segphos, reaction of indole with Ir complexes of Segphos and DM-Segphos formed an iridium product (Figure 3a) containing two hydride ligands (as determined by ^{1}H NMR spectroscopy) and one indole-derived ligand per two iridium centers. In addition, the ^{31}P NMR spectrum of the new complex contained four chemically inequivalent resonances of equal intensity.

Single crystals of the Segphos-ligated version of this complex **26** were obtained, and the structure was determined by X-ray diffraction (Figure 3b). Complex **26** results from a rare combination of N−H and C−H oxidative addition of the same substrate to two different metal centers. Complexes **26** and **27** were prepared in the absence of 1-octene, and their spectra match those of the iridium species formed in the reactions of indole with 1-octene catalyzed by Ir complexes of DM-Segphos.

The nuclearity of **25**−**27** in solution was assessed by NMR DOSY techniques. The diffusion coefficients of complexes **25**−**27** were measured under the standard catalytic reaction conditions by monitoring the hydride resonances of the metal complexes. The measured values were compared to the diffusion coefficient of the known mononuclear complex **28**

dx.doi.org/10.1021/ja412116d | J. Am. Chem. Soc. 2014, 136, 3200−3207

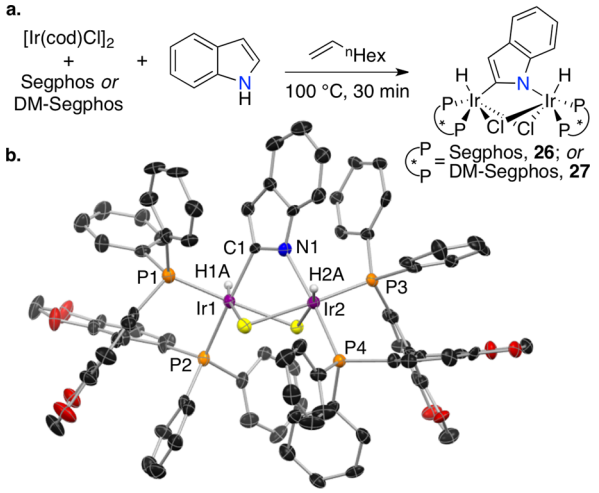

Figure 3. (a) Formation of the observed dinuclear catalyst resting state with Segphos or DM-Segphos as ligand. (b) Crystal structure of **26**.

(Figure 4a).[30] The diffusion coefficients for **26** and **27** were smaller than that for the model mononuclear complex **28**, while the diffusion coefficient of **25** was similar to that of **28**. Furthermore, DOSY NMR data for **25** were acquired with equimolar amounts of **27** (Figure 4b, left) and **28** (Figure 4b, right) present in solution as internal standards. These data are consistent with the structures for these three complexes in solution being those shown in eq 2 and Figure 3.

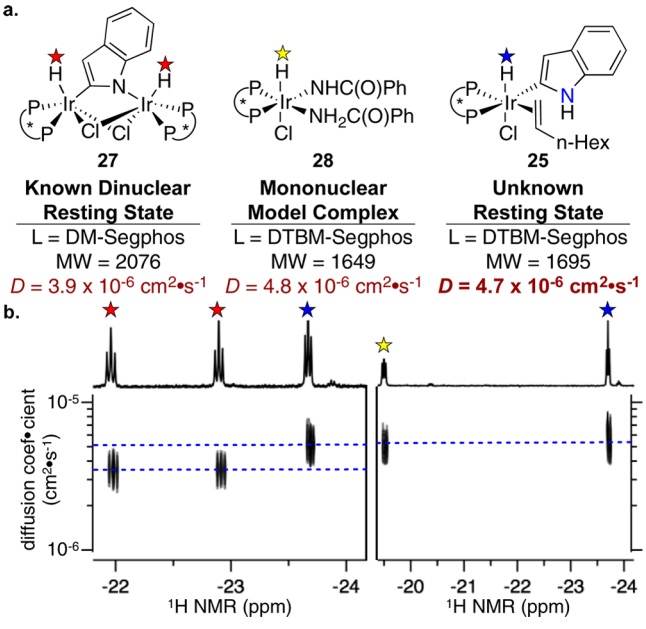

Figure 4. (a) Structures, molecular weights, and diffusion coefficients of **27**, **28**, and unknown resting state complex **25**. (b) NMR DOSY of the Ir–H region of complexes **25**, **27**, and **28**.

Kinetic Studies of a Representative Catalytic Reaction. Kinetic analysis of the addition of indole to 1-octene catalyzed by **25** was conducted by the method of initial rates (to 20% conversion). The reaction was found to be first order in catalyst and zeroth order in indole. The rate of the reaction was independent of the concentration of 1-octene under the standard catalytic conditions but depended positively on the concentration of alkene below 1.5 M. These measurements support a turnover-limiting step (TLS) that occurs from a resting-state containing a bound indolyl group and olefin.

The identity of the TLS was revealed by kinetic isotope effects (KIEs) and activation parameters. A comparison of the initial rates for the hydroamination of 1-octene with indole and 1,3-dideuteroindole in separate vessels revealed a KIE of 1.7 (Scheme 3). Although greater than unity, this KIE is likely too small to result from a turnover-limiting N–H cleavage.[19,23] This isotope effect is more consistent with reversible oxidative addition of the indole N–H bond to the Ir center prior to the TLS.

Scheme 4 shows a catalytic cycle that is consistent with our mechanistic data. The assignment of the resting state to be the

Scheme 4. Proposed Catalytic Cycle

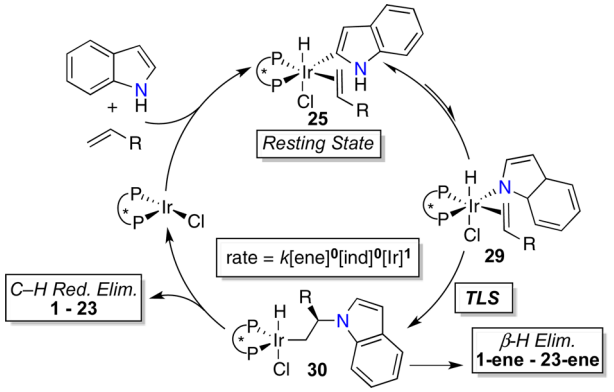

mononuclear complex **25** is based on the NMR DOSY experiments and a first-order dependence of the rate on the conentration of iridium. The deuterium-labeling experiments indicate that **25** contains a *C*-bound indolyl ligand, and $^{31}P-^{1}H$ HMBC NMR spectroscopy reveals coupling correlations between resonances of the ligand phosphorus atoms and resonances of vinylic protons of a metal-bound olefin.

The isotope effect and stereochemical study revealed the events that occur from the resting state. The KIE of 1.7 suggests that reversible isomerization of *C*-bound **25** to a less stable *N*-bound intermediate **29** occurs prior to the TLS. The stereochemistry of the vinyl indole product from the reaction of (*E*)-octene-1-d_1 (Figure 2) implied that insertion of the bound alkene into the transient *N*-bound indolyliridium complex occurs from **29**. The alkylindole product then would be generated by C–H bond-forming reductive elimination from **30**; the vinylindole product would be formed by β-H elimination from the alkyl group of **30**.

Further data on the composition of the highest energy transition state was obtained by conducting an Eyring analysis of the observed rate constants for additions of 5-fluoroindole to 1-octene at temperatures from 353 to 396 K. These data revealed the following thermodynamic parameters for the catalytic process: $\Delta H^{\ddagger}$ = 30.0 kcal/mol and $\Delta^{\ddagger}$ = 6 eu (Figure 5). The small $\Delta S^{\ddagger}$ is consistent with the same composition of the highest energy transition state as of the resting state. The highest energy transition state is likely the C–N bond formation, occurring by olefin insertion into the Ir–N bond of **29**.

Computational Studies. This reaction system provides fundamental data on rates of alkene migratory insertion into Ir–C and Ir–N bonds (Figure 6). The proposed mechanism in Scheme 4 includes olefin insertion into the Ir–N bond of **29** to

dx.doi.org/10.1021/ja412116d | J. Am. Chem. Soc. 2014, 136, 3200–3207

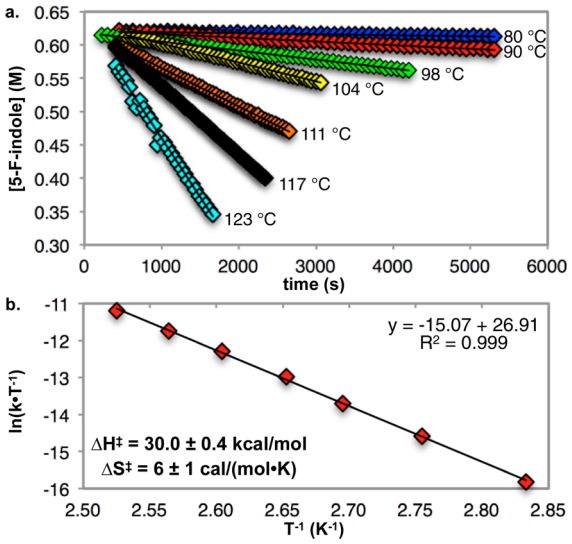

Figure 5. (a) Consumption of 5-fluoroindole vs time at variable temperatures (b) Eyring analysis of the measured rate constants.

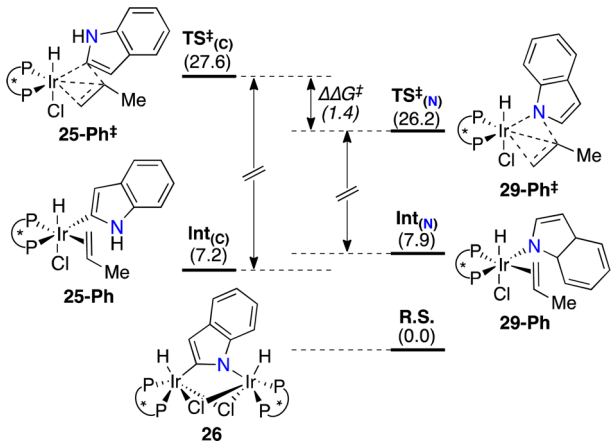

Figure 6. Depictions of the transition-state structures for olefin insertion into the Ir−C and Ir−N bond calculated by density functional theory. Free energies at 298 K are provided in parentheses.

form the observed hydroamination product, even though C-bound **25** is more stable than N-bound **29**.

To address this issue, we calculated by density functional theory (DFT) the barriers for migratory insertion reactions of analogues of **25** and **29** containing bound propene in place of 1-octene. To simplify calculations, transition states of mononuclear complexes **25-Ph**‡ and **29-Ph**‡ containing the parent Segphos ligand were modeled, rather than the systems containing the full DTBM−Segphos ligand. As previously discussed and illustrated in Figure 3, reactions catalyzed by iridium complexes of the parent Segphos ligand form a dinuclear resting state complex **26**. Thus, all calculated energies were normalized to **26**.

The calculations were conducted with the Gaussian 09 package. Geometry optimization was conducted with the M06 functionals with the lanl2dz basis set and ECP for iridium and the 6-31g(d,p) basis set for all other atoms at 298 K. Frequency analysis was conducted at the same level of theory to verify the stationary points to be minima or saddle points and to obtain the thermodynamic energy corrections. Single-point energies were calculated with the M06 functionals with the lanl2tz(f) basis set and ECP for iridium and the 6-311++g** basis set for all other atoms. Solvation in mesitylene was modeled with the IEFPCM.

Similar studies on the energy barriers for alkene insertions into late transition metal−nitrogen and metal−carbon bonds have been performed by DFT.[54] Calculations of a bisphosphine amidorhodium(I) and methylrhodium(I) complexes predicted that the barrier to ethylene insertion into the Rh−N bond of the amido complex will be lower than that for insertion into the Rh−C bond of the analogous methyl complex. These calculations suggested that a major contributing factor to the difference in rates of alkene insertion stems from the presence of a lone pair of electrons on the amido ligand. The ground state of the Rh-amido species is destabilized, relative to the analogous methyl complex, by repulsive interactions between the filled metal *d* orbital and the filled amido *p* orbital, whereas the product of insertion is stabilized by a dative Rh−N interaction. Thus, there is less Rh−N bond cleavage than Rh−C bond cleavage in the two transition states.

Results from these prior calculations on olefin insertions of rhodium(amido) and rhodium(alkyl) complexes are consistent with the lower energy for insertion of the alkene into the Ir−N indolide bond than for insertion into the Ir−C indolide bond required by the catalytic cycle in Scheme 4. However, the indolides are bound through M−C_{sp^2} and M−N_{sp^2} bonds, rather than M−C_{sp^3} and M−N_{sp^3} bonds of alkyl and amido complexes. Therefore, it is unclear whether this trend in relative rates would translate to our hydroamination of alkenes with indoles. Migratory insertion into metal aryl bonds is generally slower than insertion into metal alkyl bonds, due to the stronger metal−arene bond.[55,56] Thus, we sought to determine how the change in hybridization at nitrogen and the inclusion of the electron pair as part of an aromatic system would affect the barrier to insertion into the Ir−N bond.

All possible diastereomeric transition states of *C*-bound **25-Ph**‡ and *N*-bound **29-Ph**‡ were calculated. The barriers to propene insertion into the Ir−N bond by **29-Ph**‡ fell within a range of 26−32 kcal/mol, while barriers to insertion into the Ir−C bond by **25-Ph**‡ ranged between 28 and 33 kcal/mol. The lowest computed barrier for propene insertion into the Ir−N bond of *N*-bound indolide **29-Ph** is 1.4 kcal/mol lower than the lowest computed barrier for propene insertion into the Ir−C bond of *C*-bound indolide **29-Ph**. Although the experimental difference in energies of the system with DTBM-Segphos as ligand must be higher than 1.4 kcal/mol, the results of calculations on the truncated system with Segphos as ligand follow the trend of faster insertion into the Ir−N bond of **29** than into the Ir−C bond of **25**. These computed results parallel the trend for previously studied olefin insertions into amido- and methylrhodium complexes and support the mechanism shown in the catalytic cycle of Scheme 4.

Analysis of the optimized geometry of alkyliridium product **30-Ph** provides insight into factors that control the energy barrier for olefin insertion into *N*-indolide−iridium bonds and the relationship between this insertion reaction and the insertion into an amido complex. Interaction between iridium and nitrogen through the lone pair of electrons on nitrogen is revealed by a pyramidalization of the nitrogen atom (Figure 7). The alkyl group on nitrogen projects 40° out of the trigonal plane. As would be expected from the hybridization at nitrogen approaching sp^3, and weak interaction of the lone pair with the π-system of the indole ring, the C2−C3 bond of the indolyl fragment in **30-Ph** has more double bond character than that of

dx.doi.org/10.1021/ja412116d | J. Am. Chem. Soc. 2014, 136, 3200−3207

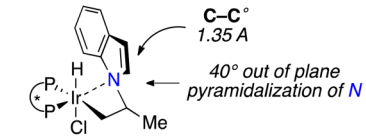

30-Ph (+11.6 kcal/mol)

Figure 7. Computed geometry of the product from propene migratory insertion into the Ir–N (**30-Ph**) by transition state **29-Ph**‡.

unbound indole. Thus, these calculations suggest that the lone pair on nitrogen is available for stabilizing interaction with iridium in the transition state, even though the starting ligand is a planar indolide with an sp^2-hybridized nitrogen.

CONCLUSIONS

In summary, we have reported a rare example of a catalytic process for the addition of the N–H bonds of indoles to simple α-olefins. This strategy for indole alkylation occurs exclusively at nitrogen. Good product yields were obtained from reactions conducted with as few as 1.5 equiv of alkene. These data reveal properties of this catalytic system that promote hydroamination of α-olefins with indoles.

1. The bulky DTBM-Segphos ligand facilitates turnover-limiting olefin insertion into the Ir–N bond.[51]
2. The bulky ligand promotes the persistence of an active mononuclear catalyst resting state, rather than off-cycle dinuclear complexes. Complexes of the less bulky Segphos and DM-Segphos ligands form dinuclear species **26** and **27**, respectively.
3. The Ir^{III} complex **25** containing a hydride, a *C*-bound indolyl ligand, and an alkene does not catalyze isomerization of the terminal alkene to less reactive internal isomers. However, bisphosphine Ir^{I} complexes do catalyze isomerization; therefore, reactions containing an Ir^{I} resting state tend to occur with a larger amount of alkene isomerization than the reaction described here.
4. The resting state contains both substrate and olefin bound to the metal center. The presence of the alkene in the resting state mitigates the requirement for conducting the reaction under conditions with neat alkene because the rate of the reaction is not dependent on the concentration of alkene.
5. The reactions occurring with less formation of vinylindole side product occur in higher ee than those occurring with more formation of the vinylindole side product. The vinyl indole is reduced in situ to the opposite enantiomer of the product than the alkyl indole formed directly from hydroamination.

Efforts to mitigate oxidative amination processes and increase the enantioselectivity of the reaction are in progress.

ASSOCIATED CONTENT

Supporting Information

Experimental procedures and characterization of all new compounds including NMR spectroscopy data, conditions for HPLC separations on a chiral stationary phase, kinetic studies, optimization data, and CIF. This material is available free of charge via the Internet at http://pubs.acs.org.

AUTHOR INFORMATION

Corresponding Author

jhartwig@berkeley.edu

Notes

The authors declare no competing financial interest.

ACKNOWLEDGMENTS

This work was supported by the Director, Office of Science, of the U.S. Department of Energy under Contract No. DE-AC02-05CH11231 and the Molecular Graphics and Computation Facility at UC Berkeley supported by the National Science Foundation (CHE-0840505). We thank Johnson-Matthey for a generous gift of $[Ir(cod)Cl]_2$, and Takasago for a generous gift of (*S*)-DTBM-Segphos. C.S.S. thanks the NSF and the Springborn family for graduate research fellowships.

REFERENCES

(1) Bagley, M. C.; Dale, J. W.; Merritt, E. A.; Xiong, X. *Chem. Rev.* **2005**, *105*, 685.
(2) Kim, J.; Movassaghi, M. *Chem. Soc. Rev.* **2009**, *38*, 3035.
(3) Joule, J. A.; Mills, K. *Heterocyclic Chemistry*; John Wiley & Sons: New York, 2010.
(4) Sundberg, R. J.; Katritzky, A. R.; Meth-Cohn, O.; Rees, C. S. *Indoles*; Elsevier Science: Waltham, MA, 1996.
(5) Bandini, M.; Melloni, A.; Umani-Ronchi, A. *Angew. Chem., Int. Ed.* **2004**, *43*, 550.
(6) Bandini, M.; Melloni, A.; Tommasi, S.; Umani-Ronchi, A. *Synlett* **2005**, 1199.
(7) Bandini, M.; Eichholzer, A. *Angew. Chem., Int. Ed.* **2009**, *48*, 9608.
(8) Stanley, L. M.; Hartwig, J. F. *Angew. Chem.* **2009**, *121*, 7981.
(9) Cui, H.-L.; Feng, X.; Peng, J.; Lei, J.; Jiang, K.; Chen, Y.-C. *Angew. Chem., Int. Ed.* **2009**, *48*, 5737.
(10) Trost, B. M.; Fleming, I. *Comprehensive Organic Synthesis: Reduction*; Elsevier Science & Technology Books: Waltham, MA, 1991.
(11) Robinson, B. *Chem. Rev.* **1969**, *69*, 785.
(12) Heaney, H.; Ley, S. V. *J. Chem. Soc., Perkin Trans. 1* **1973**, 499.
(13) Hartwig, J. F. In *Organotransition Metal Chemistry: From Bonding to Catalysis*; University Science Books: Sausalito, CA, 2010; Vol. *1*, p 700.
(14) Müller, T. E.; Hultzsch, K. C.; Yus, M.; Foubelo, F.; Tada, M. *Chem. Rev.* **2008**, *108*, 3795.
(15) Hesp, K. D.; Stradiotto, M. *ChemCatChem* **2010**, *2*, 1192.
(16) Hannedouche, J.; Schulz, E. *Chem.—Eur. J.* **2013**, *19*, 4972.
(17) Hong, S.; Marks, T. J. *Acc. Chem. Res.* **2004**, *37*, 673.
(18) Dunne, J. F.; Fulton, D. B.; Ellern, A.; Sadow, A. D. *J. Am. Chem. Soc.* **2010**, *132*, 17680.
(19) Hesp, K. D.; Tobisch, S.; Stradiotto, M. *J. Am. Chem. Soc.* **2010**, *132*, 413.
(20) Julian, L. D.; Hartwig, J. F. *J. Am. Chem. Soc.* **2010**, *132*, 13813.
(21) Shen, X.; Buchwald, S. L. *Angew. Chem., Int. Ed.* **2010**, *49*, 564.
(22) Leitch, D. C.; Platel, R. H.; Schafer, L. L. *J. Am. Chem. Soc.* **2011**, *133*, 15453.
(23) Liu, Z.; Yamamichi, H.; Madrahimov, S. T.; Hartwig, J. F. *J. Am. Chem. Soc.* **2011**, *133*, 2772.
(24) Ryu, J.-S.; Li, G. Y.; Marks, T. J. *J. Am. Chem. Soc.* **2003**, *125*, 12584.
(25) Brunet, J. J.; Chu, N. C.; Diallo, O. *Organometallics* **2005**, *24*, 3104.
(26) Karshtedt, D.; Bell, A. T.; Tilley, T. D. *J. Am. Chem. Soc.* **2005**, *127*, 12640.
(27) Zhang, J.; Yang, C.-G.; He, C. *J. Am. Chem. Soc.* **2006**, *128*, 1798.
(28) For a seminal example of asymmetric, intermolecular hydroamination of unactivated alkenes with gold, see: Zhang, Z.; Lee, S. D.; Widenhoefer, R. A. *J. Am. Chem. Soc.* **2009**, *131*, 5372.
(29) For a seminal example of asymmetric, intermolecular hydroamination of unactivated alkenes with lanthanides, see: Reznichenko, A. L.; Nguyen, H. N.; Hultzsch, K. C. *Angew. Chem., Int. Ed.* **2010**, *49*, 8984.
(30) Sevov, C. S.; Zhou, J.; Hartwig, J. F. *J. Am. Chem. Soc.* **2012**, *134*, 11960.

(31) Brunet, J.-J.; Commenges, G.; Neibecker, D.; Philippot, K. *J. Organomet. Chem.* **1994**, *469*, 221.
(32) Dorta, R.; Egli, P.; Zürcher, F.; Togni, A. *J. Am. Chem. Soc.* **1997**, *119*, 10857.
(33) McBee, J. L.; Bell, A. T.; Tilley, T. D. *J. Am. Chem. Soc.* **2008**, *130*, 16562.
(34) Zhou, J.; Hartwig, J. F. *J. Am. Chem. Soc.* **2008**, *130*, 12220.
(35) Kawatsura, M.; Hartwig, J. F. *J. Am. Chem. Soc.* **2000**, *122*, 9546.
(36) Utsunomiya, M.; Hartwig, J. F. *J. Am. Chem. Soc.* **2003**, *125*, 14286.
(37) Qian, H.; Widenhoefer, R. A. *Org. Lett.* **2005**, *7*, 2635.
(38) Pan, S. G.; Endo, K.; Shibata, T. *Org. Lett.* **2012**, *14*, 780.
(39) Nishina, N.; Yamamoto, Y. *Synlett* **2007**, 1767.
(40) Butler, K. L.; Tragni, M.; Widenhoefer, R. A. *Angew. Chem., Int. Ed.* **2012**, *51*, 5175.
(41) Löber, O.; Kawatsura, M.; Hartwig, J. F. *J. Am. Chem. Soc.* **2001**, *123*, 4366.
(42) Johns, A. M.; Sakai, N.; Ridder, A.; Hartwig, J. F. *J. Am. Chem. Soc.* **2006**, *128*, 9306.
(43) Brunet, J.-J.; Cadena, M.; Chu, N. C.; Diallo, O.; Jacob, K.; Mothes, E. *Organometallics* **2004**, *23*, 1264.
(44) Wang, X.; Widenhoefer, R. A. *Organometallics* **2004**, *23*, 1649.
(45) Cao, P.; Cabrera, J.; Padilla, R.; Serra, D.; Rominger, F.; Limbach, M. *Organometallics* **2012**, *31*, 921.
(46) Sevov, C. S.; Hartwig, J. F. *J. Am. Chem. Soc.* **2013**, *135*, 2116.
(47) Casalnuovo, A. L.; Calabrese, J. C.; Milstein, D. *J. Am. Chem. Soc.* **1988**, *110*, 6738.
(48) Liu, G.; Stahl, S. S. *J. Am. Chem. Soc.* **2007**, *129*, 6328.
(49) Hanley, P. S.; Marković, D.; Hartwig, J. F. *J. Am. Chem. Soc.*, **2010**, *132*, 6302.
(50) Neukom, J. D.; Perch, N. S.; Wolfe, J. P. *J. Am. Chem. Soc.* **2010**, *132*, 6276.
(51) Hanley, P. S.; Hartwig, J. F. *J. Am. Chem. Soc.* **2011**, *133*, 15661.
(52) Weinstein, A. B.; Stahl, S. S. *Angew. Chem., Int. Ed.* **2012**, *51*, 11505.
(53) Hanley, P. S.; Hartwig, J. F. *Angew. Chem., Int. Ed.* **2013**, *52*, 8510.
(54) Tye, J. W.; Hartwig, J. F. *J. Am. Chem. Soc.* **2009**, *131*, 14703.
(55) Garrou, P. E.; Heck, R. F. *J. Am. Chem. Soc.* **1976**, *98*, 4115.
(56) Hartwig, J. F. In *Organotransition Metal Chemistry: From Bonding to Catalysis*; University Science Books: Sausalito, CA, 2010; Vol. *1*, p 349.